Correlation between Horizontal and Vertical Ground Motions and its Effect on Structural Responses

Youichi Sono[1)], Masanori Kozuma[1)], Susumu Ino[2)], Takeshi Ugata[2)]

1) Civil Engineering Department, Kyushu Electric Power Co., Inc.
2) Nuclear Facilities Planning & Design Group, Taisei Corporation

ABSTRACT

Generally, earthquake motions are recorded as horizontal and vertical components. Since these components are derived from the same seismic source, they may have some correlations. Firstly, we evaluated and characterized correlations between horizontal and vertical components using strong-motion records observed on rock site. As a result, it was shown that the horizontal and vertical components of the observed records had some correlations, whose magnitude was related to the magnitude of earthquake. Secondly, we investigated the effects of correlations between horizontal and vertical input motions on structural responses of an outer shield. Then, it was shown that the magnitude of correlations was not related to the magnitude of structural responses, and did not have much effect on them.

INTRODUCTION

Two moderate-sized earthquakes (the 1997 Kagoshima-ken hokuseibu earthquakes) successively struck the northwestern area of Kagoshima prefecture in Japan on March 26 and May 13, 1997. Their magnitudes issued by Japanese Meteorological Agency (JMA magnitude) were 6.5 and 6.3, respectively. Epicenters of these earthquakes were about 20 km from Sendai Nuclear Power Station (NPS) site. The locations of these epicenters and Sendai NPS site are shown in Figure 1.

Sendai NPS unit 1 is instrumented with 58 channel arrays by 27 sensors as shown in Figure 2. These sensors have recorded horizontal (x and y direction) and vertical accelerations due to many earthquakes from the beginning of commercial operation. Since above two earthquakes originated nearby Sendai NPS site, we obtained peak horizontal accelerations of about 0.6 m/s^2 on the surface of rock, whose shear wave velocity was 1500 m/s [1].

We evaluated correlations between horizontal and vertical components of the observed acceleration time histories on the surface of rock, and confirmed the existence of correlation, which fluctuated depending on the events. It was considered that these correlations could not be negligible, so that we were confronted with following two problems to be solved: (1) what condition increases the correlation between horizontal and vertical components of earthquake motions, (2) to what extent does the horizontal-vertical correlation of input motions have effect on structural responses.

In order to answer the former question, we investigated relationships between horizontal-vertical correlations and seismic parameters, which were earthquake magnitude, epicentral distance and incident angle near ground surface, using the records observed during the 1997 Kagoshima-ken hokuseibu earthquakes. To answer the latter question, we investigated effects of the correlation between horizontal and vertical input motions on structural responses using the outer shield (O/S) of Sendai NPS unit 1 modeled by three-dimensional finite element (3D-FE).

EVALUATION OF CORRELATION BETWEEN HORIZONTAL AND VERTICAL COMPONENTS

Coherence Function

In order to quantify the correlation between two data sets, a coefficient of correlation is often used. However, it is important for structural responses to quantify the frequency content of the correlation. Then, we evaluate the correlation between horizontal and vertical components of strong-motion records to focus on its frequency characteristics.

In this paper, we used a coherence function to characterize the frequency content of correlation. Generally, the coherence function is used to describe incoherence between accelerations recorded at different spatial locations. It is considered that the coherence function is available to evaluation of coherency between horizontal and vertical accelerations recorded at the same point. The coherence function is defined by equation (1).

$$coh^2(\omega) = \frac{|S_{HV}(\omega)|^2}{S_{HH}(\omega) S_{VV}(\omega)} \tag{1}$$

Where $S_{HV}(\omega)$ is a cross spectrum, which is Fourier amplitude of cross-covariance function, $R_{HV}(\tau)$, between horizontal acceleration time history, $h(t)$, and vertical acceleration time history, $v(t)$. In the same manner, $S_{HH}(\omega)$ and

$S_{VV}(\omega)$ are Fourier amplitude of auto-covariance function, $R_{HH}(\tau)$ and $R_{VV}(\tau)$, respectively. The cross-covariance function, $R_{HV}(\tau)$, and the auto-covariance functions, $R_{HH}(\tau)$ and $R_{VV}(\tau)$, are defined by following equations (2) to (4).

$$R_{HV}(\tau) = E[h(t)v(t+\tau)] \tag{2}$$

$$R_{HH}(\tau) = E[h(t)h(t+\tau)] \tag{3}$$

$$R_{VV}(\tau) = E[v(t)v(t+\tau)] \tag{4}$$

Where τ is a time lag, and $E[x(t)]$ represents the mean or expected value of $x(t)$. In the case of actual acceleration time history or digital data recorded as Δt time interval, for example, the equation (2) is numerically calculated as follows:

$$R_{HV,j} = \frac{1}{N}\sum_{m=1}^{N} h_m v_{m+j} \tag{5}$$

Where N is the number of samples and h_m is m-th sample of the digital data, so that the time lag, τ, becomes $j \times \Delta t$. Finally, we can derive a cross-correlation function, ρ_j, from equations (2) to (4).

$$\rho_j = \frac{R_{HV,j}}{\sqrt{R_{HH,j}R_{VV,j}}} \equiv \frac{\sum_{m=1}^{N} h_m v_{m+j}}{\sqrt{\sum_{m=1}^{N} h_m{}^2 \sum_{m=1}^{N} v_m{}^2}} \tag{6}$$

The cross-correlation function has the similar functional form of the coherence function, and it can also quantify the horizontal-vertical correlation. The former is expressed in the time domain, while the latter is in the frequency domain. Each function is defined as

$$-1 \le \rho_j \le 1 \ , \ 0 \le coh^2(\omega) \le 1 . \tag{7}$$

For the case of completely independent horizontal and vertical motions, the value of these functions becomes zero. On the contrary, for the case of perfect correlation, the absolute value of these functions becomes one.

Evaluation of Correlation between Horizontal and Vertical Records

For our investigations, we used the major events in mainshock-aftershock sequences of the 1997 Kagoshima-ken hokuseibu earthquakes from the first mainshock to the end of 1999. A peak horizontal acceleration at the top of Reactor Building (R/B) base mat due to these events surpasses 0.02 m/s^2. Parameters of thirty-six events used for the evaluation of correlation are listed in Table 1. Where, M_j is a JMA magnitude, and M_W is a moment magnitude. The values of M_W exceeding about 3.5 are issued by NIED (National Research Institute for Earth Science and Disaster Prevention) in EMABSW (Earthquake Mechanism Analysis using Broadband Seismic Waveforms) conducted under Freesia Project. The other values of M_W are calculated from M_j using relations between M_j and M_W [3], [4].

For the evaluation of correlation between horizontal and vertical ground motions, we used acceleration time histories observed at the top of tank base mat (see Figure 2) as rock outcrop motions [1]. In order to reduce the influence of noise, we use five seconds data after S-wave arrival.

Examples of cross-correlation function and coherence function evaluated are shown in Figure 3. The coherence functions are filtered by Parzen's window of 1.0 Hz bandwidth. For the example of low correlation in the left figure, the cross-correlation does not have any significant peak, and the coherence function is almost less than 0.5. On the other hand, for the high correlation case in right figure, the cross-correlation has a peak near the time lag of zero, and the correlation function is larger than 0.5 in most of frequency range.

Relationships between Correlation and Seismic Parameters

As can been seen in Figure 3, both high and low correlations are found in the observed horizontal and vertical acceleration time histories. Then, we try to confirm what seismic parameter makes high correlation observable.

In this study, we choose three parameters as a magnitude of earthquake, M_W, an epicentral distance, Δ, which are often used as parameters of attenuation relations, and an incident angle near ground surface, θ. The characteristics of earthquake motion can be separated into three parts, which are source characteristics, propagation characteristics in the earth's crust and those in the ground near site. It is considered that M_W, Δ and θ represent these three earthquake characteristics, respectively. The third parameter, the incident angle near the ground surface of Sendai NPS site, was estimated in literature [2]. The results by ray theory in literature [2] suggest that the incident angle near ground surface may be affected by the propagation characteristics in ground near site.

The cross-correlation function and coherence function between horizontal and vertical ground motions are evaluated on both X- and Y-vertical planes, because horizontal acceleration time history is recorded as X and Y components. Furthermore, they vary with time lag or frequency. Thus, in this study, we introduced an index to represent the degree of correlation, which is an average coherence, $\overline{coh}$. The average coherence is a mean of the expected coherence function between X and vertical ground motions and that between Y and vertical ground motions, in the range of the lower frequency than 20 Hz, which is important for a nuclear facilities design. Thus, the average coherence can be written as:

$$\overline{coh} = \frac{E[coh_X(\omega)] + E[coh_Y(\omega)]}{2} \approx \frac{\frac{1}{20}\int_{0\mathrm{Hz}}^{20\mathrm{Hz}} coh_X(\omega)d\omega + \frac{1}{20}\int_{0\mathrm{Hz}}^{20\mathrm{Hz}} coh_Y(\omega)d\omega}{2} \tag{8}$$

The average coherences calculated for events are shown in Table 1.

Figure 4 shows relationships between the average coherence and the seismic parameters mentioned above. In this figure, results of the linear regression are also shown. A multiple correlation, R, is an index to represent the correlation between the estimated value by the linear regression and the average coherence calculated using the observed records. As the correlation between the estimated value by the linear regression and the calculated average coherence become higher, the R is close to one.

Relationships between the average coherence and earthquake magnitude have the highest R of 0.65. On the contrary, the average coherence versus epicentral distance relationships have the lowest R of 0.53. Figure 4(a) shows apparent tendency that the average coherence decreases as the earthquake magnitude decreases, while plots of the average coherences to epicentral distances are scattered in Figure 4(c). The multiple correlation, R, for the case of incident angle near ground surface is 0.58, which is in the middle of the cases of earthquake magnitude and epicentral distance.

As the results, it is suggested that correlations between horizontal and vertical ground motions are apt to be affected by the earthquake magnitude, that is focal mechanism, and do not have much relations with the wave propagation characteristics.

EFFECTS OF CORRELATION ON STRUCTURAL RESPONSES

Analysis Model and Input Wave

Next, in order to investigate the effects of correlations between horizontal and vertical input motions on structural responses, we applied artificial horizontal and vertical input motions with some correlations in a three-dimensional linear analysis model for the O/S with a dome of Sendai NPS unit 1. The thin shell element is used to discretize the O/S of Sendai NPS unit 1 as shown in Figure 5. Young's modulus and damping factor of concrete material are 30.4 kN/mm^2 and 2.9%, respectively, which are identified in literature [1]. The primary natural frequency of the analysis model is 4.05 Hz for horizontal direction and 10.3 Hz for vertical direction.

Horizontal and vertical input motions with some correlations are artificially generated for our analyses. Target spectra for the artificial input motions are shown in Figure 6. The vertical target spectrum is the half of the horizontal one, and the phase of vertical input motion is generated from horizontal one, such that the following relationship holds.

$$F_V(\omega) = S_{HV}(\omega)/F_H(\omega) \tag{9}$$

Where, $F_H(\omega)$ and $F_V(\omega)$ are the Fourier transform of the horizontal and vertical acceleration time history, $h(t)$ and $v(t)$, respectively, and $S_{HV}(\omega)$ is the cross spectrum. Since the $S_{HV}(\omega)$ is a part of the coherence function as shown in equation (1), we can generate the pair of horizontal and vertical input motions with any degree of correlation by controlling it. Figure 7 shows the cross-correlation function and the coherence function between horizontal and vertical input motions generated. Figure 7(a) is the case of low correlation ($\overline{coh}$=0.158), while (b) is the high correlation case ($\overline{coh}$=0.777). The degrees of correlation of these artificial input motions are similar to low and high correlation case that evaluated using the observed records as can been seen in Figure 3, respectively. In addition to these input motions, the perfectly correlated horizontal and vertical input motions are also used for the reference.

Analysis Results

Figures 8 and 9 show the horizontal and vertical five-percent damped acceleration response spectra at the major points as shown in Figure 5 due to the above-described artificial horizontal and vertical input motions. While the same horizontal input motion is used for all cases, the Fourier phase of the vertical input motion for Figure 9 is delayed in all frequency range by 180 degree to that for Figure 8. The coherence function of the horizontal and vertical input motions for Figure 9 is the same as that for Figure 8, because the coherence function is defined by only Fourier amplitude of auto- and cross-correlation function.

For the all case, the same artificial horizontal input motion is used, so that horizontal response spectra are similar to each other. In only Figures 8(b) and 9(b), the effect of the vertical input motion on the horizontal response spectra appears at the bottom of dome near 0.1 s (10 Hz), which is the primary natural frequency of the analysis model in vertical direction. On the other hand, there are differences among the vertical response spectra. Since the effect of error in the artificial vertical input motion generation is included in these differences, it is considered that the horizontal and vertical correlations do not have much effect on the response spectra to the degree of correlation evaluated by the observed records. Furthermore, the magnitude of correlations is not related to the magnitude of structural responses. For instance, in spite of the same coherence function, the spectral acceleration due to the perfectly correlated horizontal and vertical input motions is the highest in period of 0.1 to 0.2 s as shown Figure 8(f), while that due to the perfectly correlated horizontal and vertical input motions with inverse phase is the lowest in Figure 9(f).

CONCLUSIONS

Horizontal and vertical components of the observed records on ground surface of Sendai nuclear power station site due to the 1997 kagoshima-ken hokuseibu earthquakes had some correlations. Coherence function between horizontal and vertical ground motions decreased as the earthquake magnitude decreased. Therefore, it was suggested that the magnitude of the correlations was related to the focal mechanism.

Next, in order to investigate effects of the correlations between horizontal and vertical input motions on structural responses, artificial horizontal and vertical input motions with some correlations were applied in a three-dimensional finite element model for the outer shield of Sendai nuclear power station unit 1. Then, we obtained different response spectra due to the artificial horizontal and vertical input motions with different phase and the same coherence function. Furthermore, the structural responses were not much affected by correlation between horizontal and vertical input motions to the degree of correlation evaluated by the observed records. These results suggest that not only the correlation between horizontal and vertical input motions, but also phase characteristics of the input motions are important for structural responses due to simultaneously input in horizontal and vertical direction.

ACKNOWLEDGEMENTS

The authors are grateful to Dr. Tohru Masao for the generating technique of artificial earthquakes with correlation between horizontal and vertical components.

REFERENCES

1. Kinoshita,Dai, Sono,Youichi, Kiyohara,Kazuhiko, Masao,Tohru, Ugata,Takeshi and Kodama,Joji, Earthquake Observation and Simulation Analysis of Sendai Nuclear Power Station on the 1997 Kagoshima-Ken Hokuseibu Earthquakes, SMiRT-15, K07/3, 1999, pp.VIII.281-288
2. Sigaki,Takahiro, Kiyohara,Kazuhiko, Sono,Youichi, Kinoshita,Dai, Masao,Tohru, Tamura,Ryoichi, Yochimura,Chiaki and Ugata,Takeshi, Estimation of Earthquake Motion Incident Angle at Rock Site, 12WCEE, 2000, 0956
3. Kanamori,H., The Energy Release in Great Earthquakes, J. Geophys. Res., Vol.82, 1981, pp.2981-2987
4. Fukushima,Yoshimitsu and Tanaka,Teiji, Scaling Relations for Earthquake Source Spectrum and JMA Magnitude, Journal of Stract. Constr. Engng, AIJ, No.425, 1991, pp.19-25 (in Japanese)

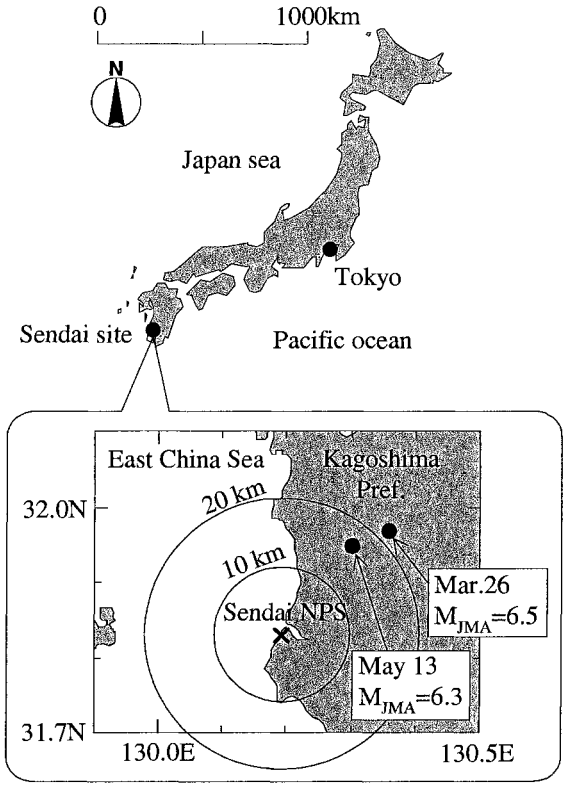

Fig.1 Location of Sendai NPS site and epicenter of mainshocks

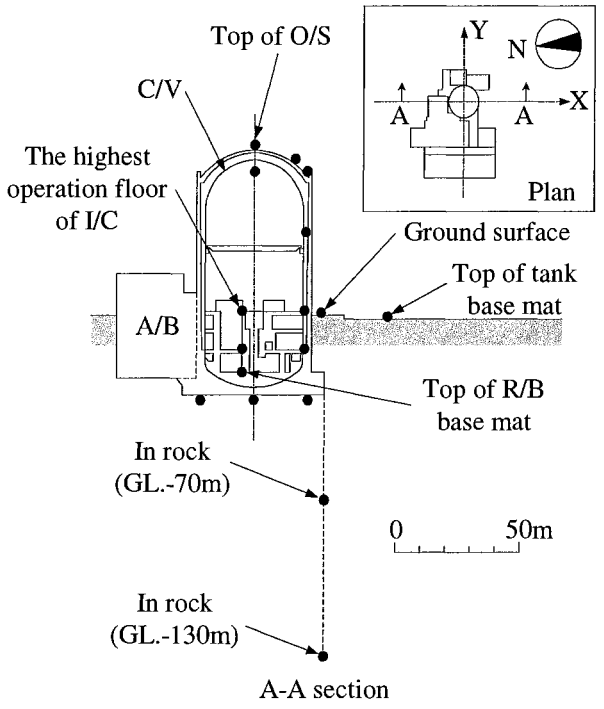

Fig.2 Sensor locations

Table 1 List of main aftershocks (included mainshocks) and their average coherence

Event	Date	Time in Japan	M_j	M_W	h (km)	Δ (km)	θ (°)	$\overline{coh}$	Event	Date	Time in Japan	M_j	M_W	h (km)	Δ (km)	θ (°)	$\overline{coh}$
1	1997/3/26*	17:31	6.5	6.1	11.8	22.0	42.8	0.346	19	1997/11/11	21:41	3.2	3.6	9.5	17.1	38.6	0.480
2	1997/3/26	18:05	4.4	4.6	13.0	25.1	46.9	0.317	20	1997/12/14	0:19	3.5	3.8	8.9	9.6	20.5	0.577
3	1997/3/26	22:24	4.3	4.7	9.3	28.1	46.9	0.372	21	1997/12/25	0:17	3.9	4.0	6.5	9.2	20.5	0.507
4	1997/3/26	22:48	3.4	3.7	9.5	20.9	42.8	0.552	22	1997/12/25	18:58	3.4	3.7	7.4	9.2	28.5	0.507
5	1997/3/31	9:04	3.6	3.8	8.1	20.4	50.5	0.394	23	1998/1/10	14:01	3.7	3.9	6.1	8.8	28.5	0.602
6	1997/4/3	4:33	5.6	5.4	14.8	19.7	28.5	0.462	24	1998/1/10	14:02	4.1	4.4	6.5	8.8	NC	0.514
7	1997/4/3	5:13	3.4	3.7	8.5	19.8	33.6	0.608	25	1998/3/3	8:30	3.8	3.9	7.8	9.5	NC	0.577
8	1997/4/4	2:33	4.6	4.7	14.3	23.8	33.6	0.352	26	1998/3/3	16:39	3.7	4.0	8.2	9.4	NC	0.475
9	1997/4/5	13:24	4.8	5.0	12.0	25.3	42.8	0.311	27	1998/3/27	15:31	4.1	4.4	9.0	29.6	NC	0.422
10	1997/4/9	23:20	4.8	4.8	10.5	26.1	38.6	0.329	28	1998/3/27	15:33	3.9	4.1	9.0	29.8	NC	0.409
11	1997/4/9	23:23	4.5	4.6	9.0	27.1	50.5	0.370	29	1998/4/13	13:37	3.7	3.9	7.8	9.9	NC	0.374
12	1997/4/15	9:33	3.3	3.6	8.8	19.9	33.6	0.552	30	1998/4/15	11:50	3.4	3.7	8.7	9.3	NC	0.471
13	1997/5/3	9:00	3.5	3.6	9.0	20.0	33.6	0.480	31	1998/4/18	1:22	3.6	3.9	9.1	9.5	NC	0.472
14	1997/5/13*	14:38	6.3	6.0	9.2	16.5	42.8	0.270	32	1998/4/20	10:50	3.9	4.3	10.1	30.8	NC	0.370
15	1997/5/14	8:32	4.7	4.9	8.9	18.6	42.8	0.332	33	1999/1/12	0:45	3.6	3.9	8.9	10.5	NC	0.436
16	1997/5/25	6:11	4.2	4.3	8.1	18.2	65.7	0.406	34	1999/4/3	3:45	4.1	4.3	8.0	18.2	NC	0.417
17	1997/6/27	14:12	4.0	4.1	8.7	21.7	38.6	0.364	35	1999/7/31	7:55	4.0	4.0	10.7	15.2	NC	0.413
18	1997/7/26	18:36	4.2	4.3	9.1	27.9	NC	0.394	36	1999/11/20	18:46	3.2	3.6	9.7	11.8	NC	0.413

M_j: JMA magnitude, M_W : moment magnitude, h : focal depth, Δ : epicenter distance, θ : incident angle,
$\overline{coh}$: average coherence defined by equation (8), NC : not calculated, * : mainshock

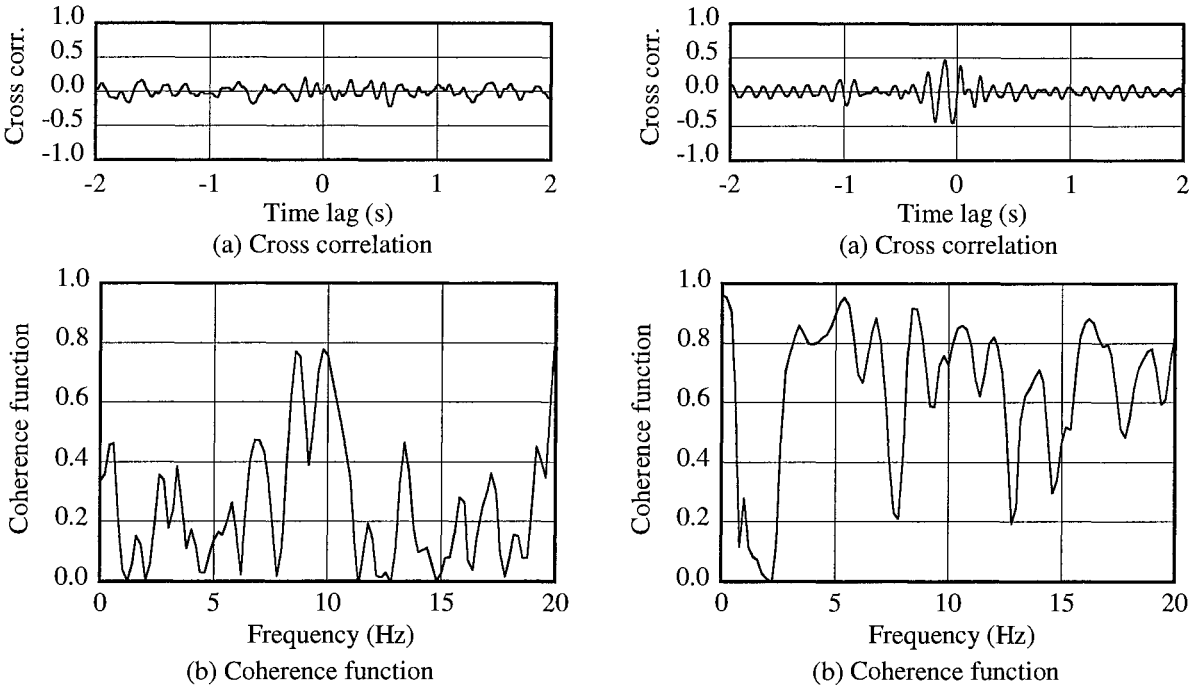

Fig.3 Examples of cross correlation and coherence function. Left figure shows low coherency (Event 14), and right is high coherency (Event 7).

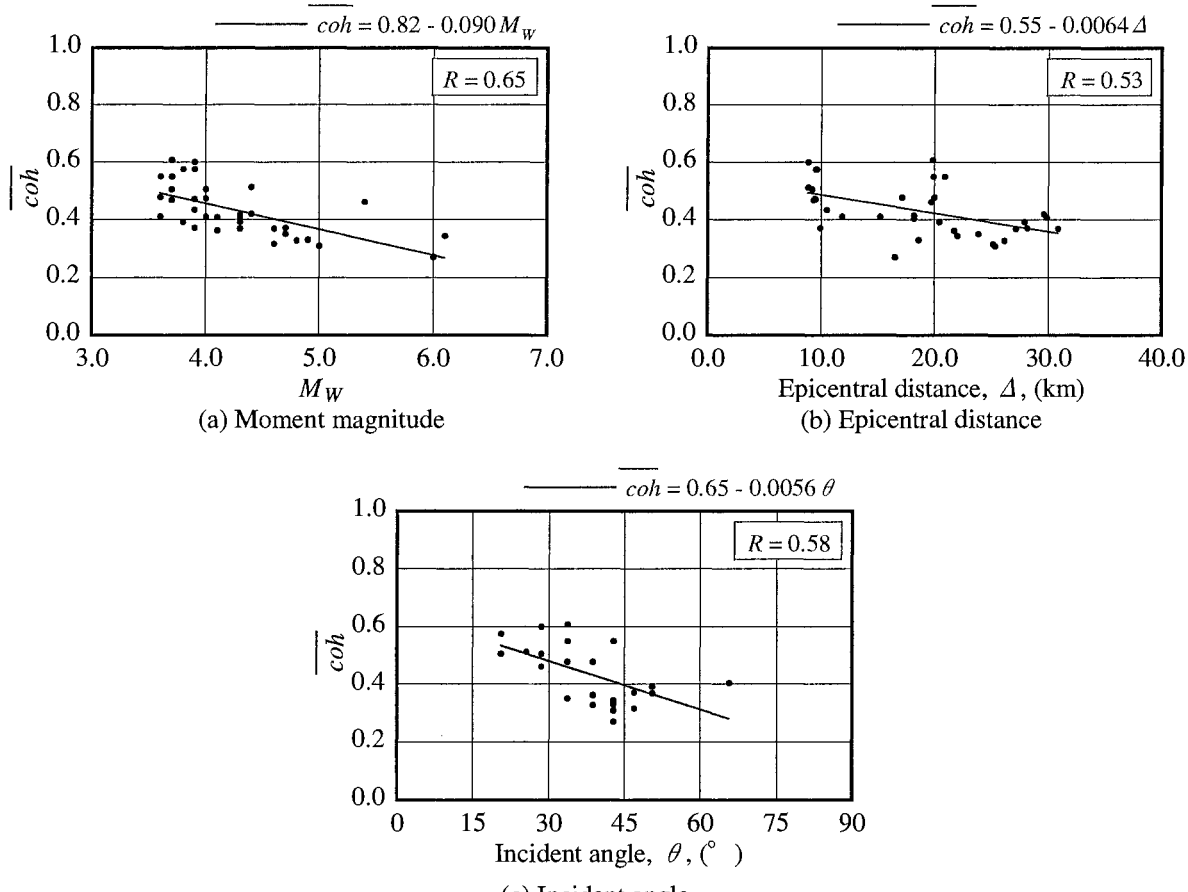

Fig.4 Relationships between seismic parameters and average coherence

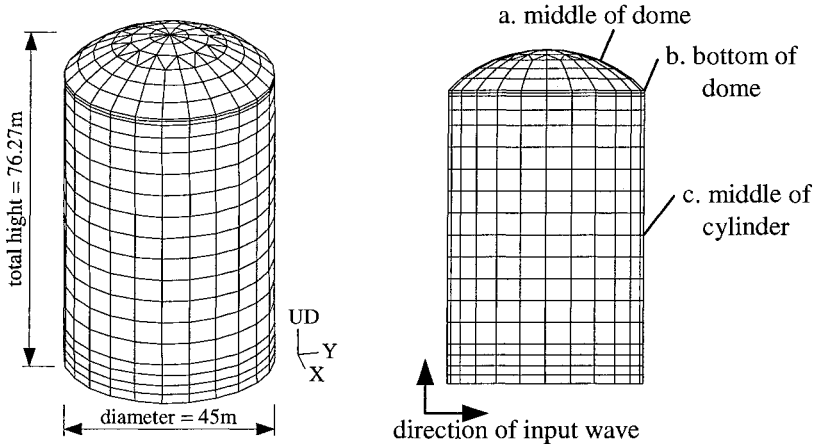

Fig.5 Analysis model

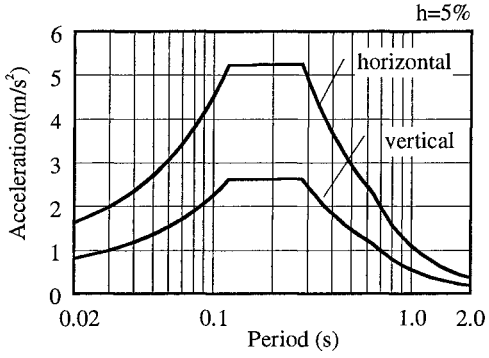

Fig.6 Target spectra of artificial input waves

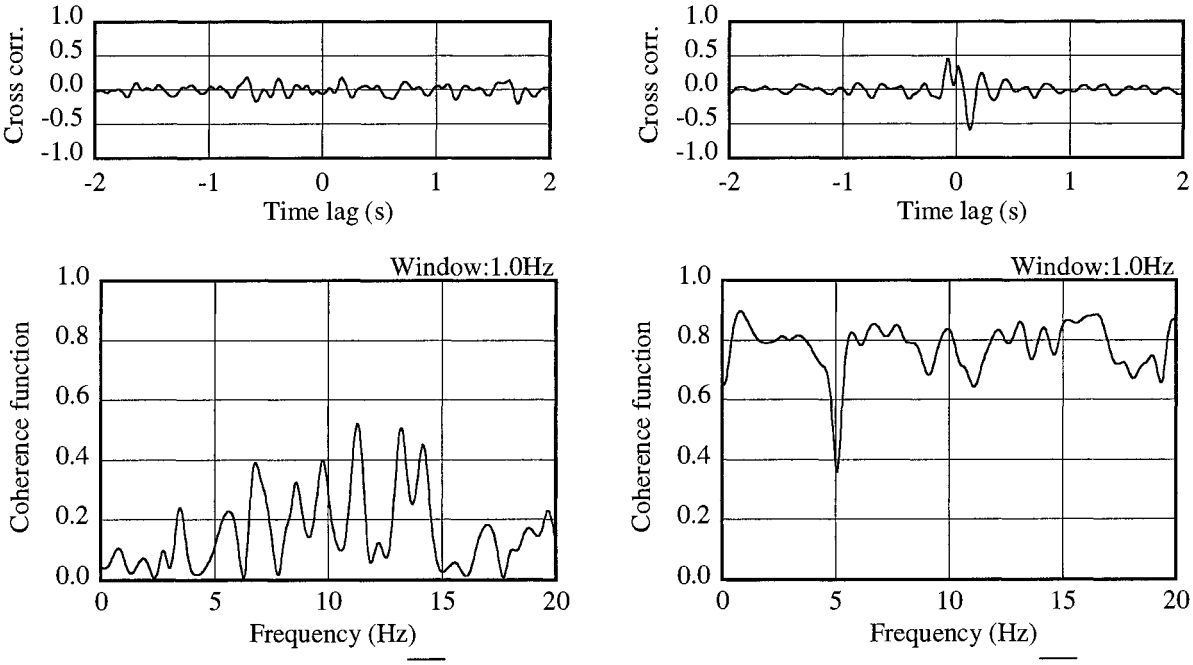

(a) Low correlation wave ($\overline{coh}$ =0.158) (b) High correlation wave ($\overline{coh}$ =0.777)

Fig.7 Cross correlations and coherence functions of artificial horizontal and vertical input motions

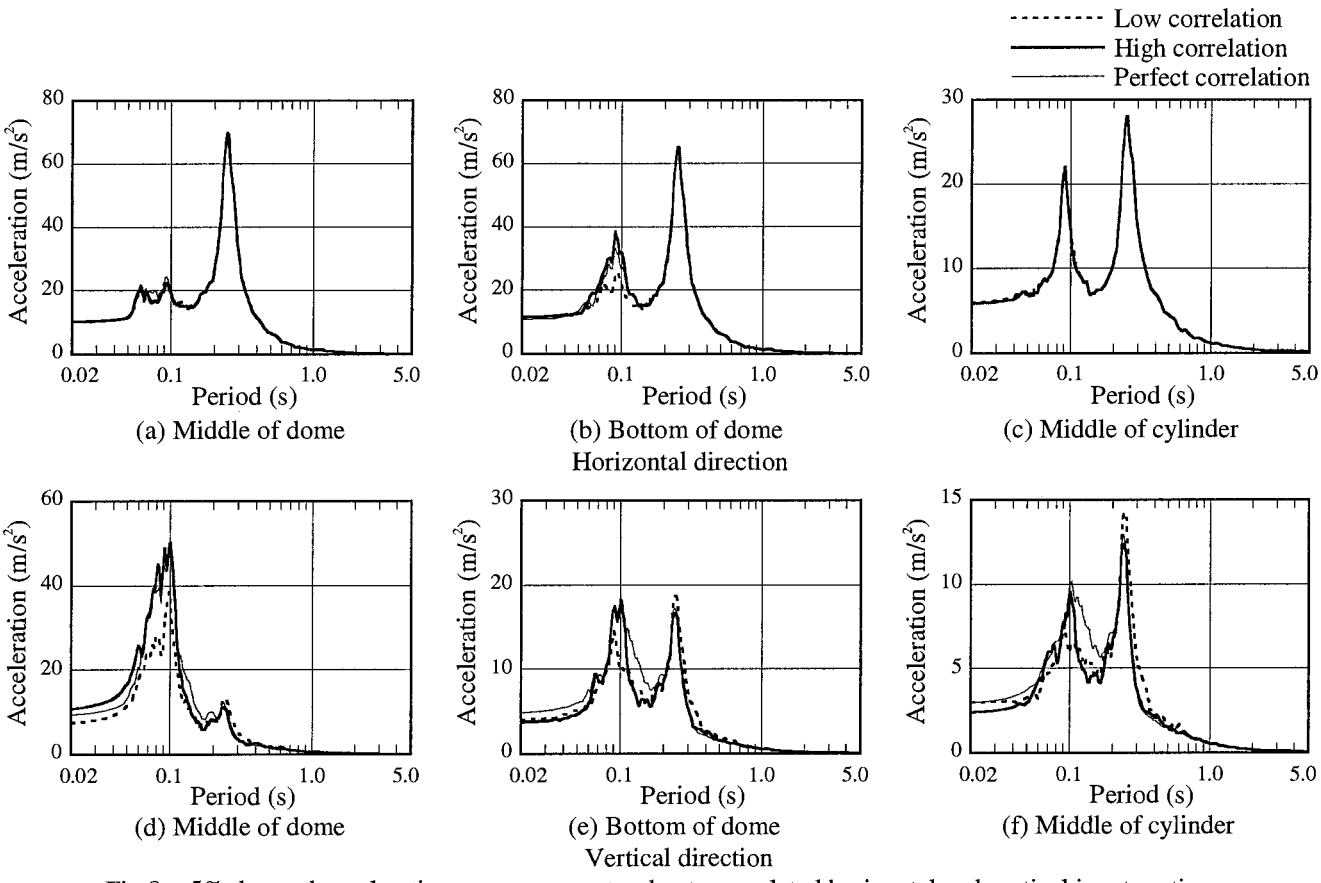

Fig.8 5% damped acceleration response spectra due to correlated horizontal and vertical input motions

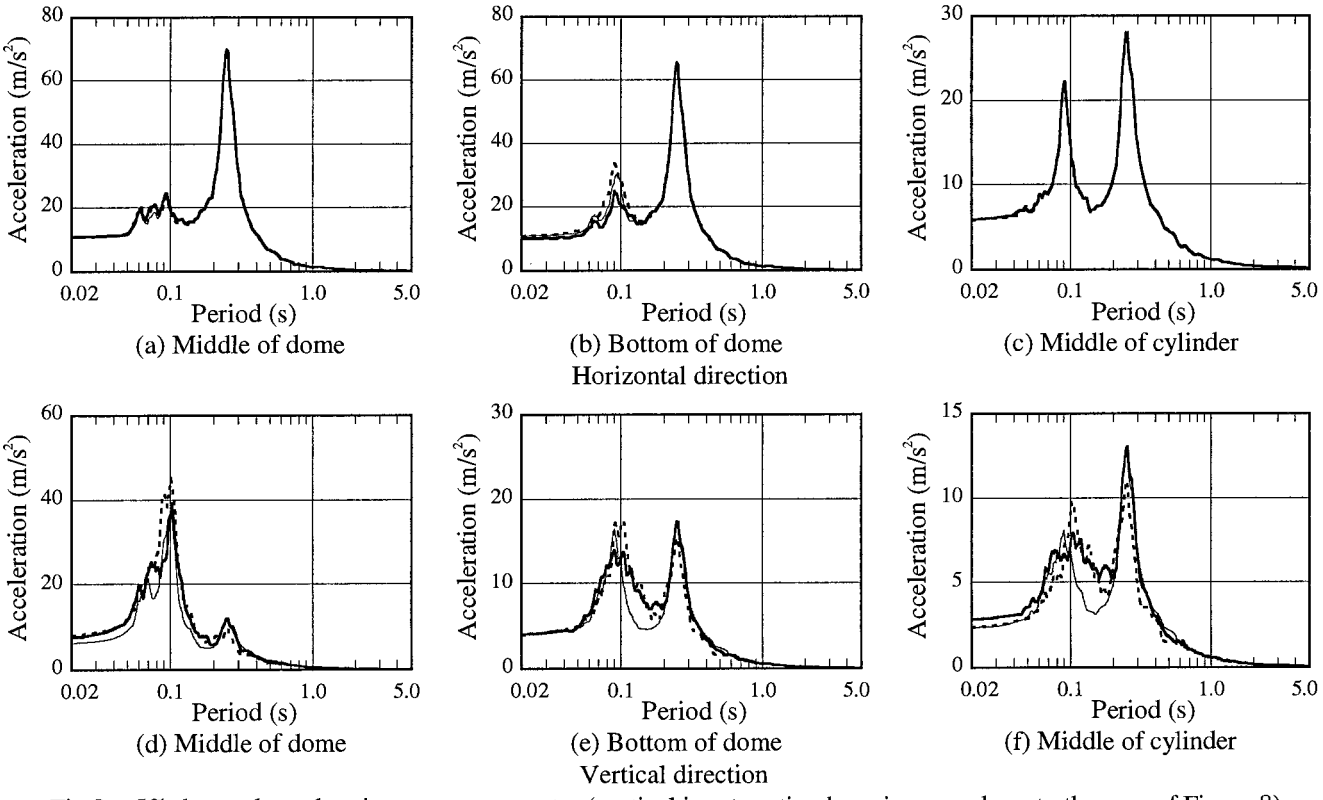

Fig.9 5% damped acceleration response spectra (vertical input motion have inverse phase to the case of Figure 8)